Electronic Supplementary Material (ESI) for RSC Advances.

Understanding and Improving Assays for Cytotoxicity of Nanoparticles: What really matters? – Supplementary information

Methods

A schematic showing an overview of the whole study is presented herein:

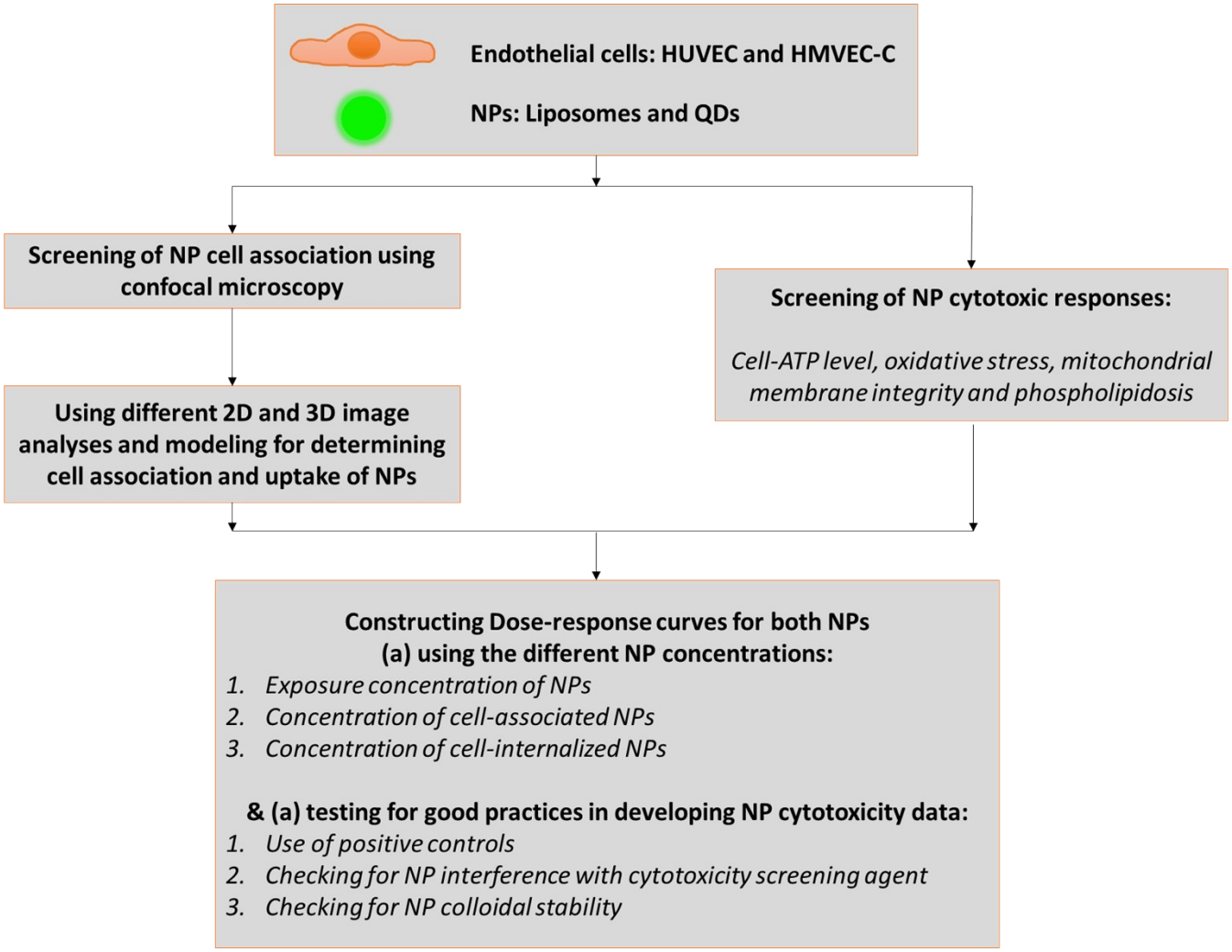

Cell association study of liposomes using other Fluorescence-based techniques

Colloidal stability of nanoparticles in presence of cells

Colloidal stability of liposomes (0.8-8nM) in terms of size and PDI was tested in presence of cells following 24h exposure at 37°C. Blank culture media, as well as, 8nM liposomal dispersion

in culture media (not exposed to cells) were used as controls and were denoted as non-treated and treated controls, respectively.

Cell-nanoparticle association experiment

HUVEC and HMVEC-C were seeded in gelatin-coated 12-well plates at a cell density of 11400 and were grown to confluency. Oregon-green-labelled liposomes in culture medium at a concentration range of 0.08-8nM were filter-sterilized through 0.2 μm polycarbonate membrane and incubated with cells for 24 h at 37°C.

Both HUVEC and HMVEC-C were seeded separately in gelatin-coated 12-well plates (Sigma Aldrich, St. Louis, Missouri, USA) at a cell density of 11400 cells/well and were grown to confluence. Oregon-green-labelled liposomes were dispersed in culture medium just before the experiment and were filter-sterilized through 0.2 μm polycarbonate membrane. Liposomes (2ml/well) with a concentration range of 0.08-8nM were incubated with cells for 24 h at 37°C. Fluorescence-based techniques were used to analyse the liposome-containing culture media after and before cell incubation as well as cell lysate after exposure to liposomes. Blank culture media and blank culture media-treated cell lysate were used as controls. The total protein content was also determined.

Cell lysis

On collection of the culture media, cells were rinsed twice with PBS to get rid of the remaining culture media containing non-associated liposomes, and lysed using a volume of 1 ml/well of 1μL/mL tritonX-100 in PBS. Cell lysates were collected for further analysis.

Fluorescence plate reader measurements

SpectraMax M2 plate reader (Molecular devices, Sunnyvale, California, USA) was used to measure the fluorescence of non-associated liposomes in the collected culture media following the cell-liposome association experiment, and that of associated liposomes in cell lysate in black-walled 96-well plates (Sigma Aldrich, St. Louis, Missouri, USA). Excitation and emission wavelengths were set to 501nm and 526nm, respectively. Control measurements of liposomes in culture media before incubation with either cells were done for comparison. Concentrations were determined reference to the appropriate calibration curves.

Fluorescence correlation spectroscopy (FCS)

FCS is a powerful more sensitive technique for monitoring the concentration of non-associated liposomes based on the analysis of intensity fluctuation of labelled liposomes at nanomolar concentration in a femtoliter volume (10^{-15}). Control liposomal dispersions before cell incubation were used as controls.

An upright Zeiss Axiovert 200 (Mississauga, ON, Canada) microscope with a 40x water immersion objective lens (1.2 NA and 0.8mm working distance) was used to record fluorescence. Two photon excitation (TPE) was achieved using a mode-locked Ti: Sapphire, 100fs pulsed laser (Tsunami, Spectra Physics, Palo Alto, CA, United States) operating at 82MHz and 780nm with a power of 30 mW. The excitation beam was expanded using a Galilean telescope to optimally fill the back of the objective lense. This set-up resulted in an estimated TPE volume (Ve) of approximately 2.508×10^-15L. Fluorescence emission from the fluorophores was collected through the same objective lens and reflected off a dichroic optic (Chroma 100DCSPXr, Rockingham, Vermont), which separated the emitted fluorescence from

the excitation source. A second optic (Chroma 565DCLP) separated the red and green fluorescence of the fluorophore. The spectrally separated emissions were passed through band-pass filters (Chroma, D535/50x (green), D605/40m (red)) before they were directed using optical fibers to Si avalanche photodiodes (APD, Perkin-Elmer, SPCQ-200, Freemont, CA). The signal from the APDs was analyzed using a correlator board (ALV5000／E, Langen, Germany). The resulting data was analyzed using Origin Pro 2015 software.

Bicinchoninic acid assay (BCA)

Pierce BCA Protein Assay Kit (Thermo Scientific, Rockford, Illinois, USA) was used to measure the protein concentration of each experimental replicate reference to a calibration curve of standard bovine serum albumin supplemented with the kit and aliquoted to have a concentration range of 250 to 2000 µg/ml. A total of three 25µL samples were analyzed for each well. The assay was followed according to the manufacturer's instructions and absorbance at 562 nm was measured in 96 well-plates (Thermo Scientific, Waltham, Massachusetts, USA) using SpectraMax M2 plate reader (Molecular devices, Sunnyvale California, USA).

Confocal imaging and image analysis

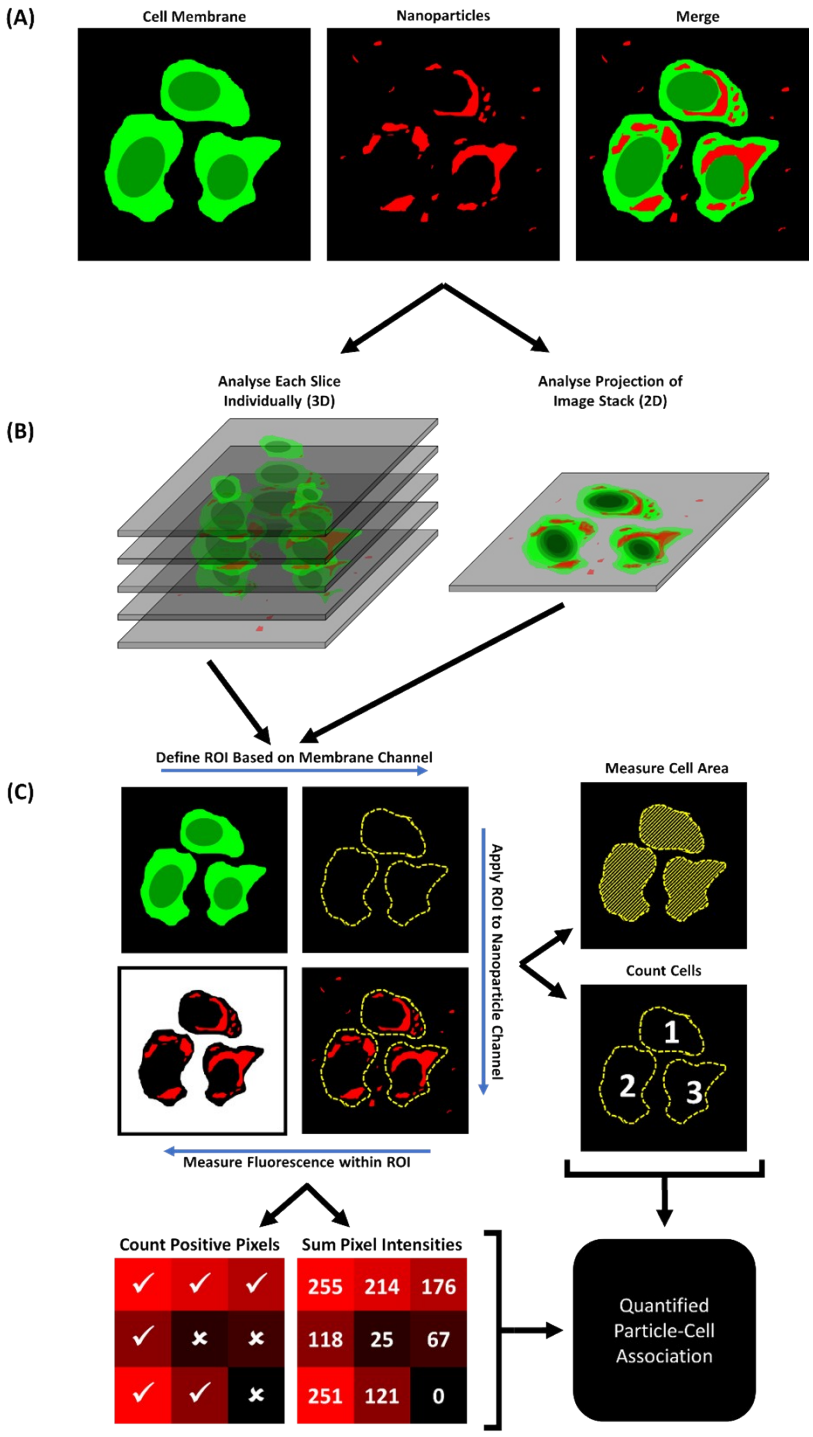

Figure S1: Schematic flow summarizing all the image analysis approaches adopted to determine nanoparticle association using confocal microscopy. (A) Images of the cell membrane (green) and nanoparticles (red) were sequestered at different positions in z direction to develop a Z-stack. (B) Each slice of the z-stack analyzed. Alternatively, a z-projection image was developed using ImageJ. (C) Region of interest (ROI) was then defined using the cell membrane channel and applied to the nanoparticle channel to quantify the fluorescent signals of cell-associated nanoparticles based on their intensities or pixel counts. In order to normalize nanoparticle

association by either of cell area and cell number, Image J was used to determine the area of cells islet and cells were counted manually.

3D Reconstruction of the confocal z-stacks: cell internalization of nanoparticles

A 3D reconstruction of the confocal z-stacks were generated using image processing software ScanIP Simpleware (Synopsys). A diagram summarizing the workflow is presented in Figure S2. Spacing parameters were defined from image acquisition specifications as 1.240, 1.240, and 1.242 μm/pixel for x, y and z, respectively.

Membrane channel images were thresholded to select the cell membrane: A region of interest for the images showing the membrane channel was defined by adjusting the threshold values for the minimum and maximum greyscale values accepted, in general, the threshold for the cell membrane was defined between greyscale values of 18 to 35 for 8-bit images. Each image of the analyzed stack was checked from different views, x-y (top view) and x-z and y-z (lateral cross-sections) to verify that only the membrane region was selected.

A mask containing all the voxels in the membrane volume was created. Additionally, masks for the whole cell volume and for the intracellular volume were defined. NP-track images were thresholded to select the pixels due to NPs. Post processing filters were applied to remove background noise when needed.

NP adhesion and internalization were quantified in terms voxel numbers and fluorescence intensities within the cell membrane and cell interior volumes, respectively. Results normalized by the total cells volume were presented as mean ± standard deviation.

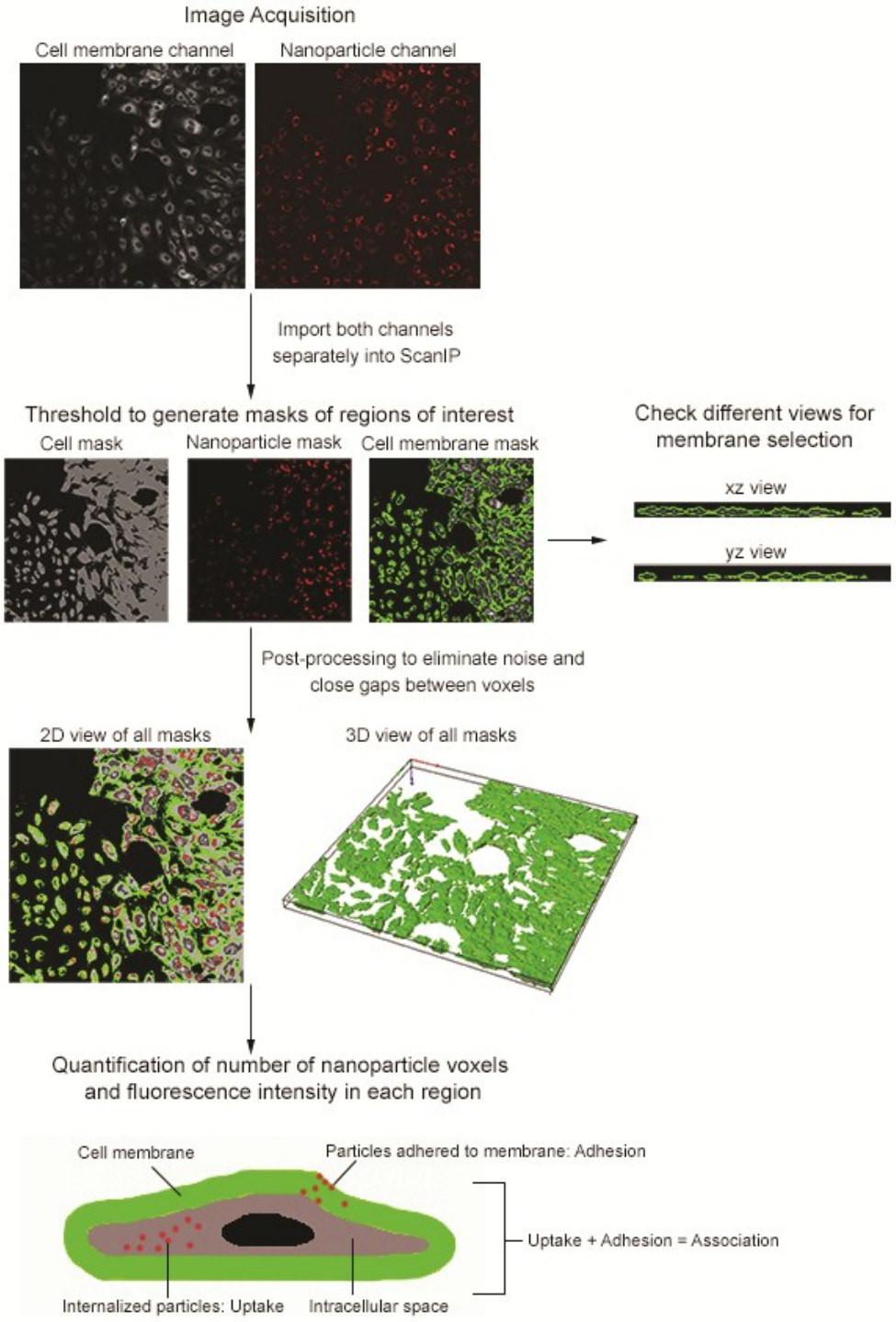

Figure S2: Schematic summarizing the workflow for generation of 3D model of sequestered Z-stacks using ScanIP Simpleware and quantification of adhered and internalized nanoparticles. Steps are discussed in more details in the methods section in the main manuscript.

Statistical analysis of cell NP association and internalization data

One-way/Two-way ANOVA and posthoc-Tukey HSD test were used for statistical analysis. The assumptions of no outliers, normality and homogeneity of variances were tested by generating boxplots of the residuals, Shapiro-Wil test of normality, and Levene's test for equality of variances, respectively. For heteroskedastic data, comparison was done using a weighted least squares regression. Differences are considered significant at $p<0.05$.

Cytotoxicity study

Cell viability assay

ViaLight™ Plus is an ATP bioluminescent assay kit that measures cytoplasmic adenosine triphosphate (ATP) to assess the functional integrity of living cells. This bioluminescent assay utilizes the enzyme luciferase to catalyze the formation of light from ATP and luciferin. The emitted light intensity is linearly related to ATP concentration [1]. Assay was conducted reference to manufacturer's recommendations. Bioluminescence was measured (SpectraMax M2 plate reader, Molecular devices, Sunnyvale, California, USA). Cells grown in culture medium only were considered as negative control (100% cell viability) and others incubated with Triton X-100 (1µL/mL) were used as positive control (0% cell viability). Cells underwent irreversible permeabilization of the membrane and structural collapse on exposure to Triton X-100 (non-ionic surfactant) at postmicellar concentration and lose cytoplasmic ATP [2]. Percentage cell viability was calculated based on five replicates as follows:

$$\%\ Cell\ viability = \frac{Lum_{exp} - Lum_{positive\ control}}{Lum_{negative\ control} - Lum_{positive\ control}} * 100 \qquad \textit{Equation 1}$$

ATP controls in concentrations of 1.5 and 0.015µM were prepared. 50µl of each of the control and each of the NPs were incubated together with 100µl ATP monitoring reagent Plus®. Bioluminescence was measured to check for wavelength interference in absence of cells.

Assays for specific intracellular mechanisms for potential nanoparticle cytotoxicity

Interference assays. In absence of cells, either of MitoHealth, CellROX, LipidTOX reagents were prepared as recommended by the manufacturer and mixed with NPs (4-8nM liposomes or 100-200nM quantum dots) in 96 well plates (ThermoFisher Scientific, Waltham, MA, USA). The 96 well plates were incubated at 37°C for the time recommended in the assay, 30min (MitoHealth and CellROX) or 24h (LipidTOX), then measured for fluorescence (SpectraMax M2 plate reader, Molecular Devices, Sunnyvale, California, USA) using excitation/emission wavelengths of 544/590nm (MitoHealth) or 485/538 nm (CellROX and LipidTOX) and compared to fluorescence of a control reagent solution in culture media. A significant difference ($P > 0.05$) in fluorescence measurement from control solution implies that test nanoparticles interfered with the assay reagent.

CellROX Oxidative Stress assay. Oxidative stress is induced when the cell is provoked into producing excessive reactive oxygen species. The production of reactive oxygen species can lead to many detrimental effects, such as inducing oxidative DNA and mitochondrial damage and is an early indicator of potential cell death. [3] CellROX Green reagent is a fluorogenic probe measuring reactive oxygen species in live cells. The cell-permeable reagent has weak fluorescence in the reduced state and upon oxidation exhibit strong fluorogenic signal. Upon oxidation, it binds to DNA; thus, its signal is primarily localized in the nucleus and mitochondria [4].

Assay was conducted as recommended by the supplier. Plates were imaged immediately using fluorescence microscope (Olympus IX 71, Olympus Corporation, Tokyo, Japan) using a FITC filter. For each experimental trial, a minimum of four replicates were conducted with three images per well were sequestered. Images were then analyzed using image J freeware. Images were first thresholded to remove background noise, then mean fluorescence intensity was analyzed. Mean fluorescence intensity per cell number was then determined. An increased signal corresponds to cells undergoing increased levels of oxidative stress. Cells grown in culture medium only were considered as negative control (0% oxidative stress) and others incubated with menadione (100µM) were used as positive control (100% oxidative stress) being reported to induce the generation of reactive oxygen species [5, 6]. Percentage cells undergoing oxidative stress (% *Oxid. Stress*) using the following equation:

$$\% \, Oxid. Stress = \frac{F_{exp} - F_{negative\ control}}{F_{positive\ control} - F_{negative\ control}} * 100 \qquad \textit{Equation 2}$$

Where:
F_{exp}: Mean fluorescence intensity per cell number of test sample.
$F_{negative\ control}$: Mean fluorescence intensity due to cells not experiencing oxidative stress; exposed to culture media only.
$F_{positive\ control}$: Mean fluorescence intensity due to cells treated with menadione to induce oxidative stress.

Mitochondrial health assay. The mitochondrial membrane potential (MMP) is a central feature of healthy mitochondria and is essential for ATP synthesis through the mitochondrial respiratory chain. MMP dysfunction was quantified with HCS Mitochondrial Health Kit (Invitrogen, Carlsbad, CA, USA). The Mitochondrial Health Kit uses two dyes: the MitoHealth stain accumulates in the mitochondria of live cells proportional to the mitochondrial membrane potential, Hoechst 33342 stains nuclear DNA in live and dead cells. Assay was conducted as recommended by the manufacturer. Fluorescence intensity was measured using a SpectraMax

M2 plate reader (Molecular Devices, Sunnyvale, California, USA) at 544/590 nm (MitoHealth stain) and normalized for nuclei at 355/460 nm , with a cutoff at 455 nm (Hoechst 33342). Cells grown in culture medium only were considered as negative control (100% MMP) and others incubated with tolcapone (20 µM) were used as positive control (0% MMP). Percentage mitochondrial membrane potential (% MMP) of cultured cells is determined using the following equation:

$$\% MMP = \frac{F_{exp} - F_{positive\ control}}{F_{negative\ control} - F_{positive\ control}} * 100 \qquad \textit{Equation 3}$$

Where:

F_{exp}: Mean fluorescence intensity per cell number of test sample.

$F_{negative\ control}$: Mean fluorescence intensity due to cells not experiencing MMP reduction; exposed to culture media only.

$F_{positive\ control}$: Mean fluorescence intensity due to cells treated with tolcapone to induce MMP reduction.

Tolcapone was shown by Haasio et al [7] to reduce the mitochondrial membrane potential in a concentration-dependent manner. When using tolcapone at 12–20µM concentrations, they observed a reduction in mitochondrial membrane potential to 0–7% of the initial value. Accordingly, tolcapone (20 µM) was used as positive control for Mitohealth kit which measure the mitochondrial membrane potential.

LipidTOX™ Phospholipidosis Detection Reagents. LipidTOX™ Green detection reagent was used to test for phospholipidosis. Phospholipidosis is characterized by an excessive accumulation of intracellular phospholipids on exposure to a xenobiotic, usually a cationic amphiphilic drug, which directly interacts with cellular phospholipids, e.g. within cell membranes, or interferes with the synthesis and metabolism of phospholipids, e.g. inhibition of phospholipases.[8] Phospholipidosis is especially important to test for in case of liposomes based on their reported fusion with cell membranes. [9-11]

A volume of 100 µl of unlabelled liposomal dispersions of a series concentration of 0.08-8 nM in culture medium was tested on 80% confluent HUVEC and HMVEC-C seeded in 96-well plates (ThermoFisher Scientific, Waltham, MA, USA). Quantum dots within the concentration range 0.2-200 nM were tested in parallel. Cells were incubated with the nanoparticles for 24h at 37°C together with LipidTOX phospholipidosis detection reagent added at a final dilution of the stock solution of 1:1000 in culture medium. This was followed by the same steps for cell washing, imaging and image analysis as per CellROX protocol. An increased signal corresponds to cells undergoing increased levels of phospholipidosis. Cells grown in culture medium only were considered as negative control (0% phospholipidosis) and others incubated with propranolol (30µM) were used as positive control (100% phospholipidosis). Percentage cells undergoing phospholipidosis (% Phospholipidosis) is determined using the following equation:

$$\%\ Phospholipidosis = \frac{F_{exp} - F_{negative\ control}}{F_{positive\ control} - F_{negative\ control}} * 100 \qquad \textit{Equation 4}$$

Where:
F_{exp}: Mean fluorescence intensity per cell number of test sample.
$F_{negative\ control}$: Mean fluorescence intensity due to cells not experiencing phospholipidosis; exposed to culture media only.
$F_{positive\ control}$: Mean fluorescence intensity due to cells treated with propranolol to induce phospholipidosis.

Propranolol (30µM) was recommended by the manufacturer as a positive control for LipidTox assay, being able to induce accumulation of phospholipid [12].

Results and Discussion

Colloidal instability of NPs could be also triggered by cell milieu and cell excretions as well as the physical barrier of the cell membrane. This was further checked using labelled liposomes.

Presence of cells; HUVEC or HMVEC-C, did not elicit instability of test liposomes as shown by the insignificant difference in mean size diameters and the overlapping size distribution curves (Figure S3) in absence and presence of either of HUVEC or HMVEC-C cells. The relatively higher PDI at 1.2nM was attributed to measurement errors and insensitivity of the technique at such low liposome concentration. DLS measurements of liposomes in culture media were not possible at lower concentrations of labelled liposomes (0.8 and 0.08nM).

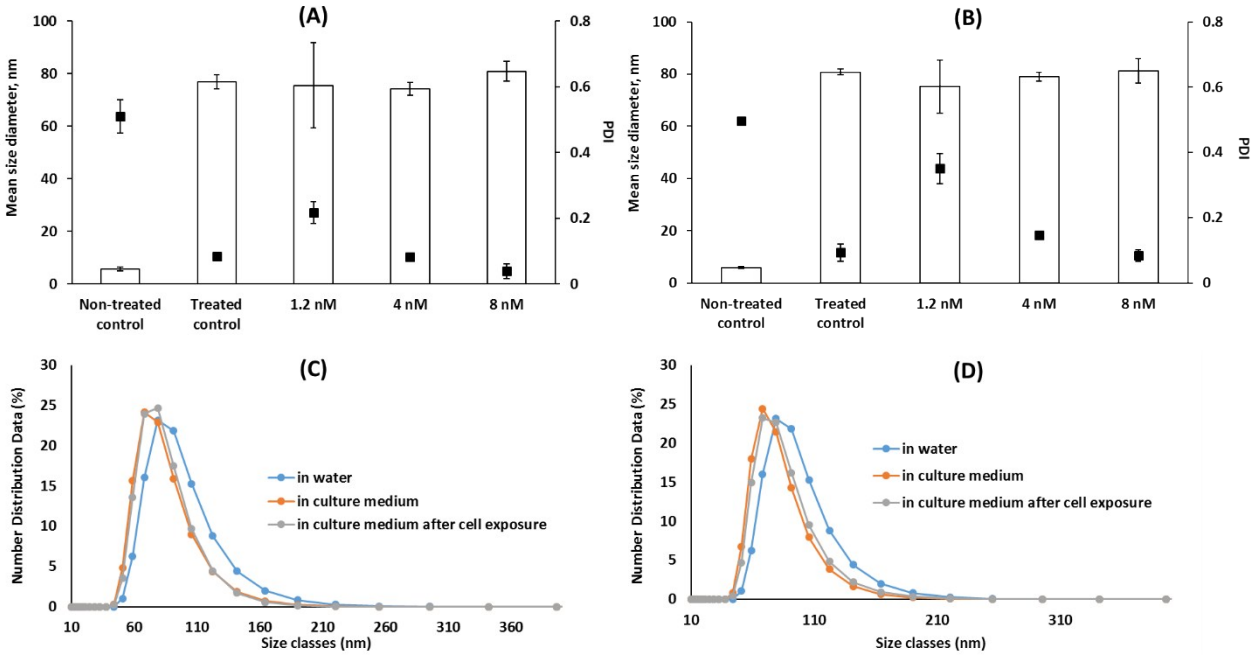

Figure S3: Colloidal stability of labelled liposomes in presence of cells; HUVEC (A, C) and HMVEC-C (B, D). Mean size diameters, depicted as bars, and polydispersity index (PDI), depicted as black squares, of liposomes (1.2, 4 and 8nM) on exposure to HUVEC (A) and HMVEC-C (B) for 24h compared to either of blank culture media (untreated controls) and 8nM liposomal dispersion in culture media in absence of cells (treated controls). Size distribution curves of 8nM labelled liposomes dispersed in water, culture media (EGM-2 and EGM-2MV) in presence and absence of cells, HUVEC (C) and HMVEC-C (D) after incubation at 37°C for 24h as determined using dynamic light scattering.

Knowing that only a small percentage of nanoparticles suspended in media could associate with the cells (aka an infinite supply system), confocal imaging produced more reliable association data than spectroscopic techniques based on depletion from the dispersion (plate-reader measurements and fluorescence correlation spectroscopy) (Figure S4). Representative confocal images are presented in Figures S5-S8 and quantitation Figures complementary to those in main manuscript are shown below (Figures S9-S13).

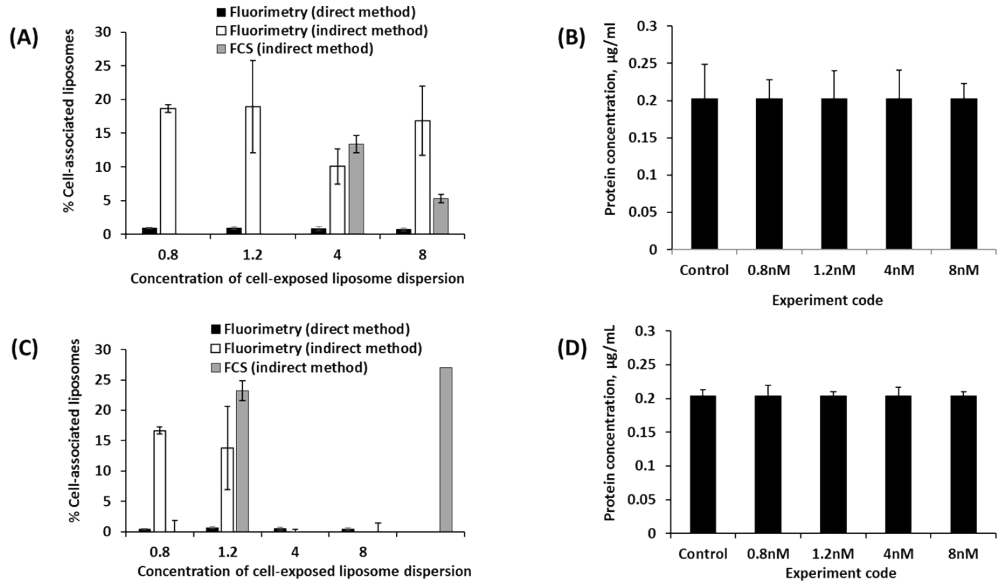

Figure S4: Conflicting results of % liposome association with HUVEC (A) and HMVEC-C cells (C) after 24h exposure as determined by fluorescence-based methods; Fluorimetry and fluorescence correlation spectroscopy (FCS). Direct methods include analysis of liposome concentration in the cell lysate. Indirect measurements are based on measurement of non-associated liposomes in the culture media. Protein concentration of cell lysate was measured in parallel. No significant difference in the protein content indicate fairly equal number of cells among experimental replicates. This eliminates cell density scatter as a factor introducing variability in the obtained cell association results of liposomes.

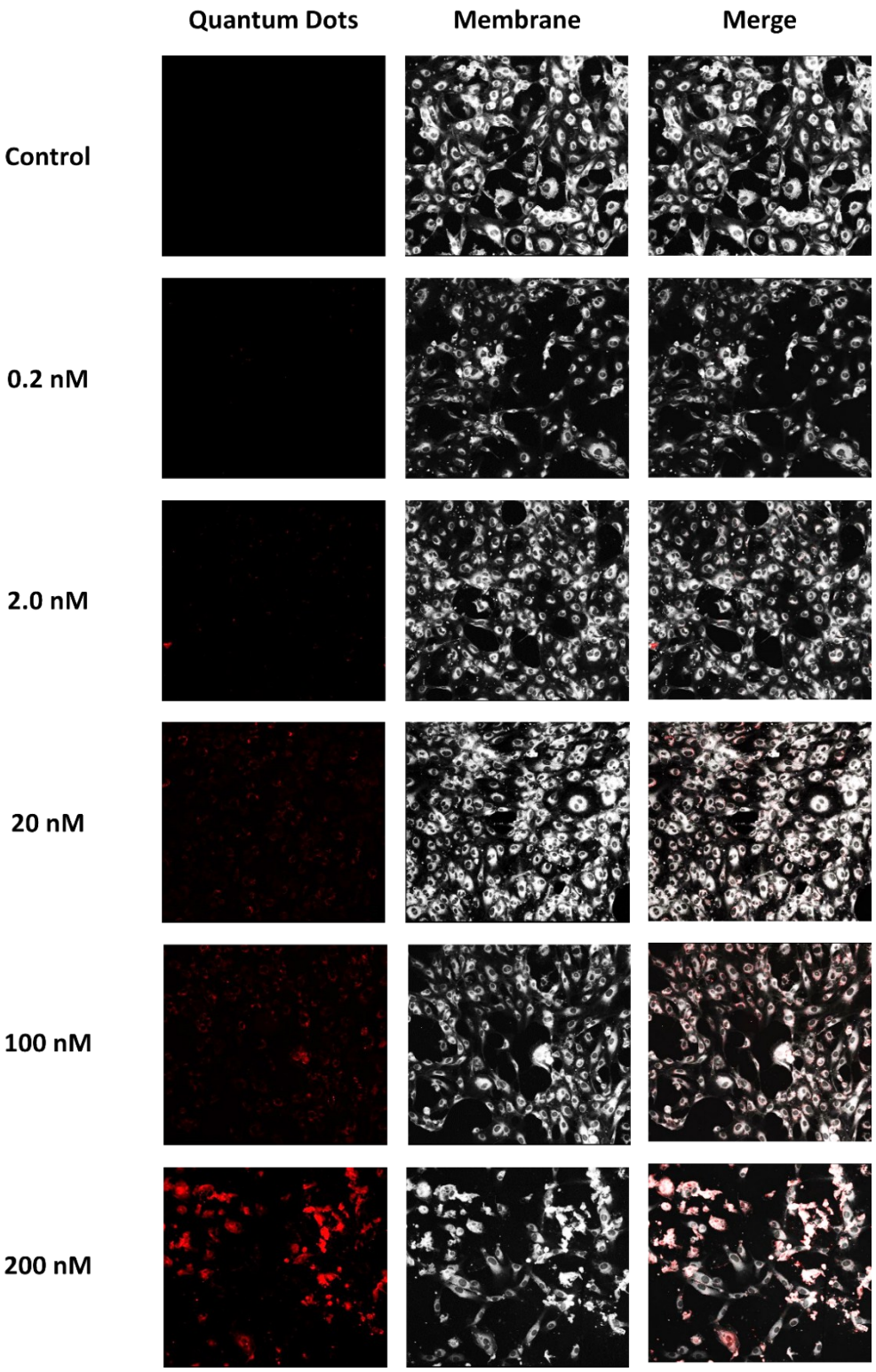

Figure S5: Quantum dots associated with HUVEC cells at different exposure concentrations (0.2-200 nM) as imaged by confocal microscopy. The figure shows representative fluorescent images (dimension: 317.331 µm x 317.331 µm) of quantum dots (red), HUVEC cells (white) and the corresponding overlaid images labelled as Merge.

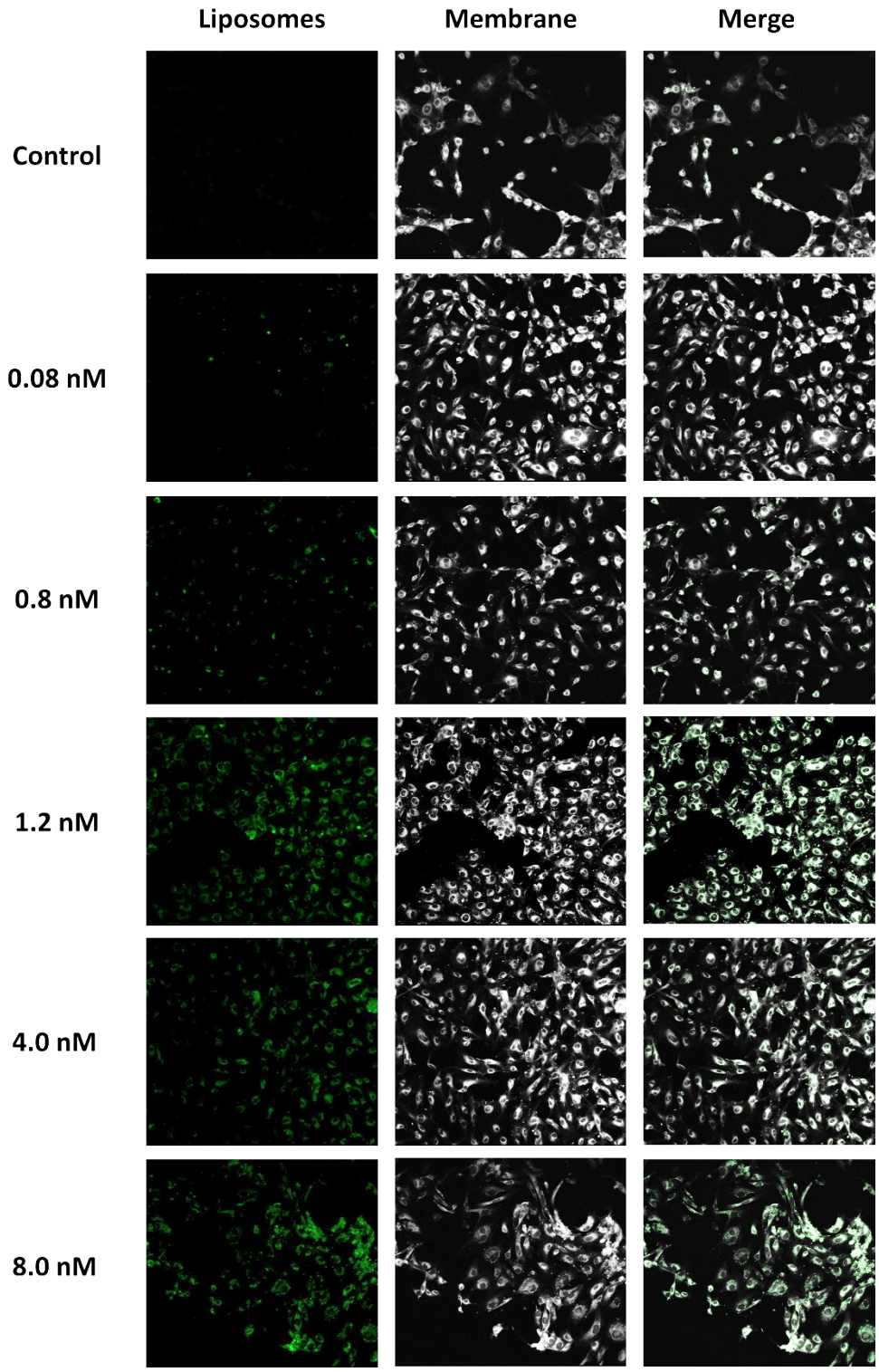

Figure S6: Liposomes associated with HUVEC cells at different exposure concentrations (0.08-8 nM) as imaged by confocal microscopy. The figure shows representative fluorescent images (dimension: 317.331 μm x 317.331 μm) of liposomes (green), HUVEC cells (white) and the corresponding overlaid images labelled as Merge.

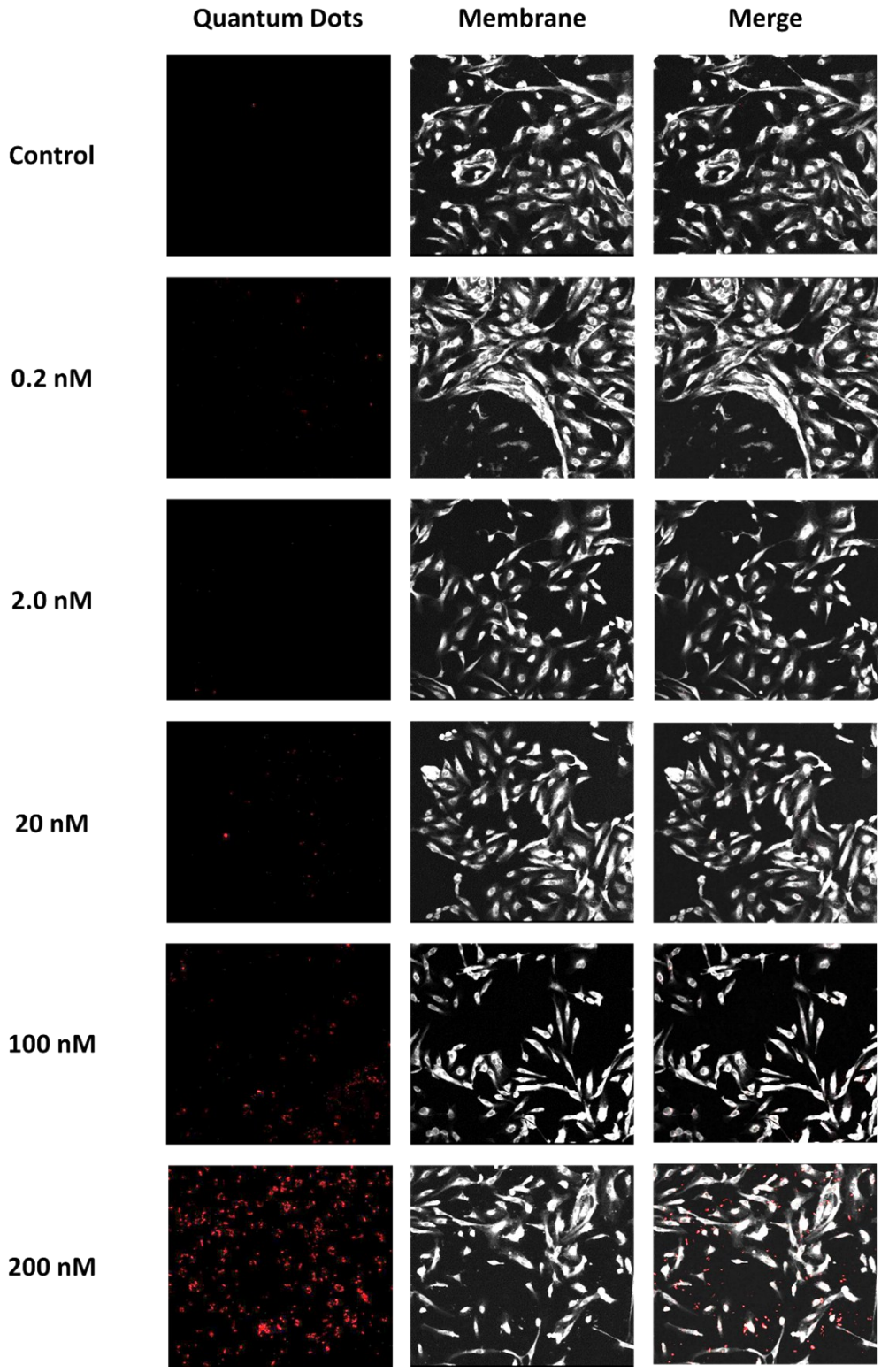

Figure S7: Quantum dots associated with HMVEC-C cells at different exposure concentrations (0.2-200 nM) as imaged by confocal microscopy. The figure shows representative fluorescent images (dimension: 317.331 µm x 317.331 µm) of quantum dots (red), HUVEC cells (white) and the corresponding overlaid images labelled as Merge.

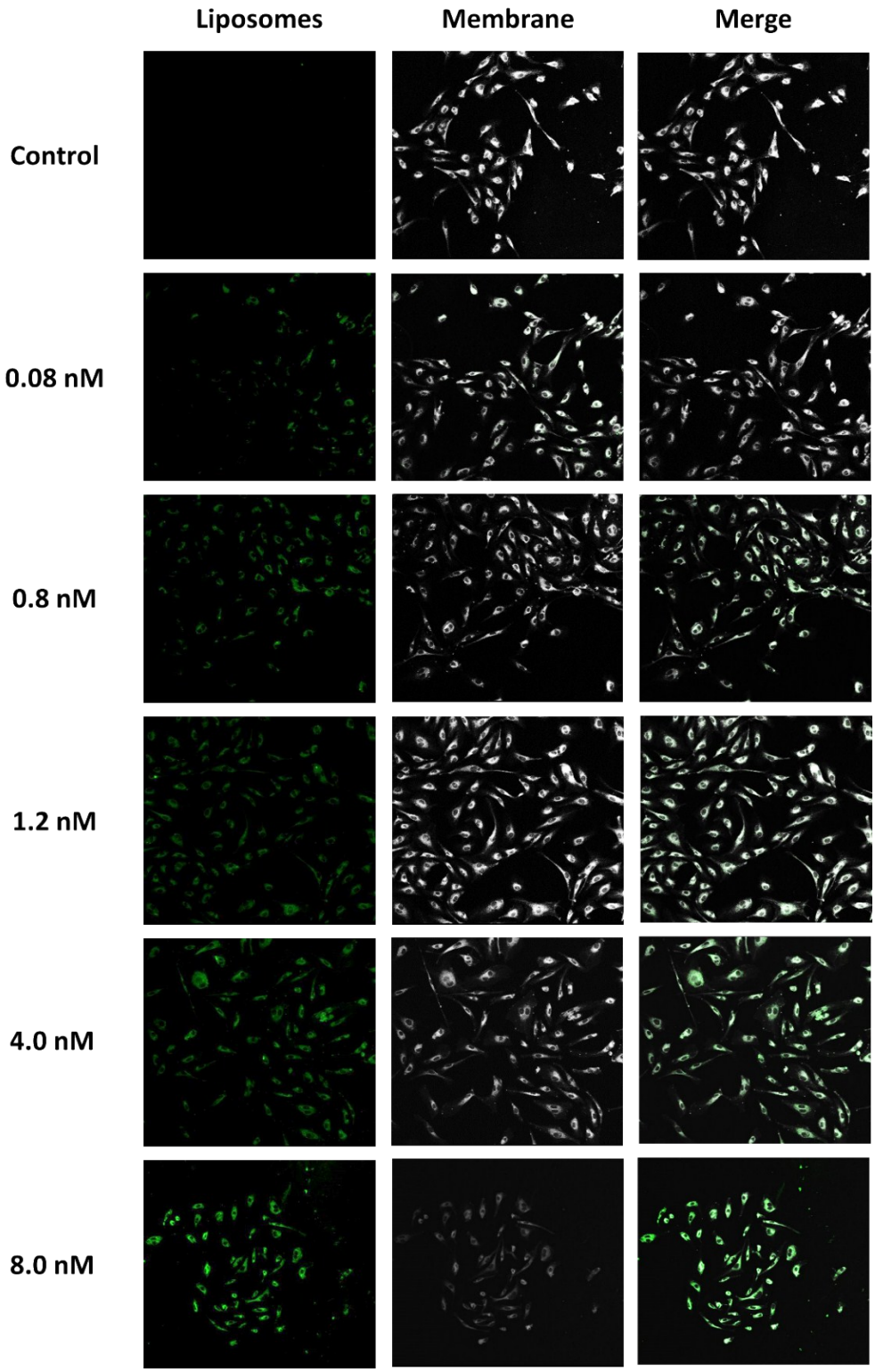

Figure S8: Liposomes associated with HMVEC-C cells at different exposure concentrations (0.08-8 nM) as imaged by confocal microscopy. The figure shows representative fluorescent images (dimension: 317.331 µm x 317.331 µm) of liposomes (green), HUVEC cells (white) and the corresponding overlaid images labelled as Merge.

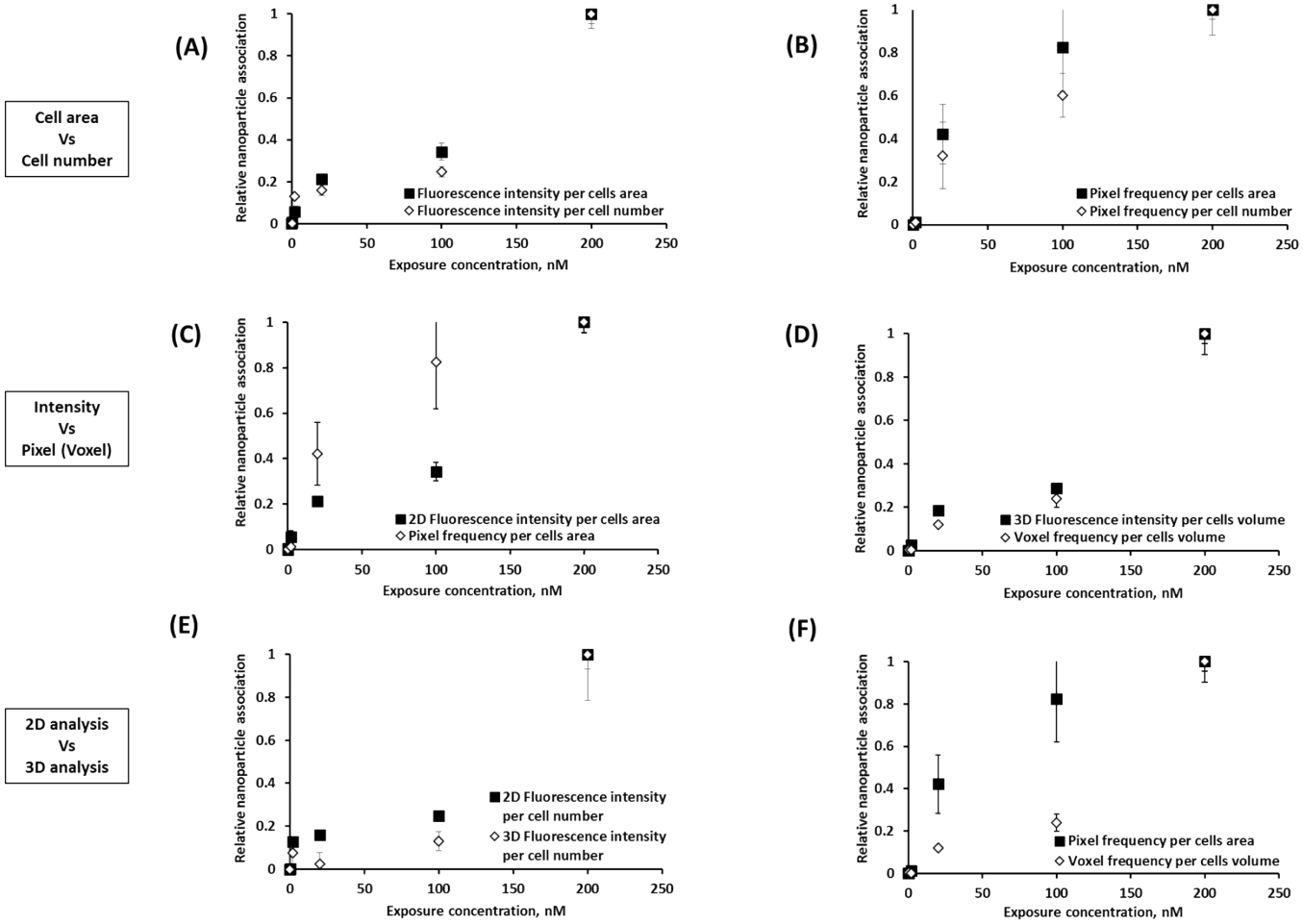

Figure S9: Effect of the method adopted for image analysis of sequestered Z-stacks on the association results of quantum dots as determined by confocal imaging on exposure to HUVEC cells for 24h at 37°C; cells area versus cell number measurements (A and B), fluorescence intensity versus pixel (C)/voxel (D) frequency, 2D versus 3D analysis (E and F). Representative images in this figure capture some of these trends: (A) 2D Fluorescence intensities per cells area and cell number. (B) Pixel frequencies per cell area and cell number. (C) 2D Fluorescence intensity and pixel frequency (per cell area). (D) 3D Fluorescence intensity and voxel frequency (per cells volume). (E) 2D and 3D Fluorescence intensities (per cells area/volume). (F) Pixel and Voxel frequencies (per cell number). Points with error bars represent mean ± standard deviation. The differences between the two curves in panels C, E and F are statistically significant (Two-way ANOVA, $p<0.05$).

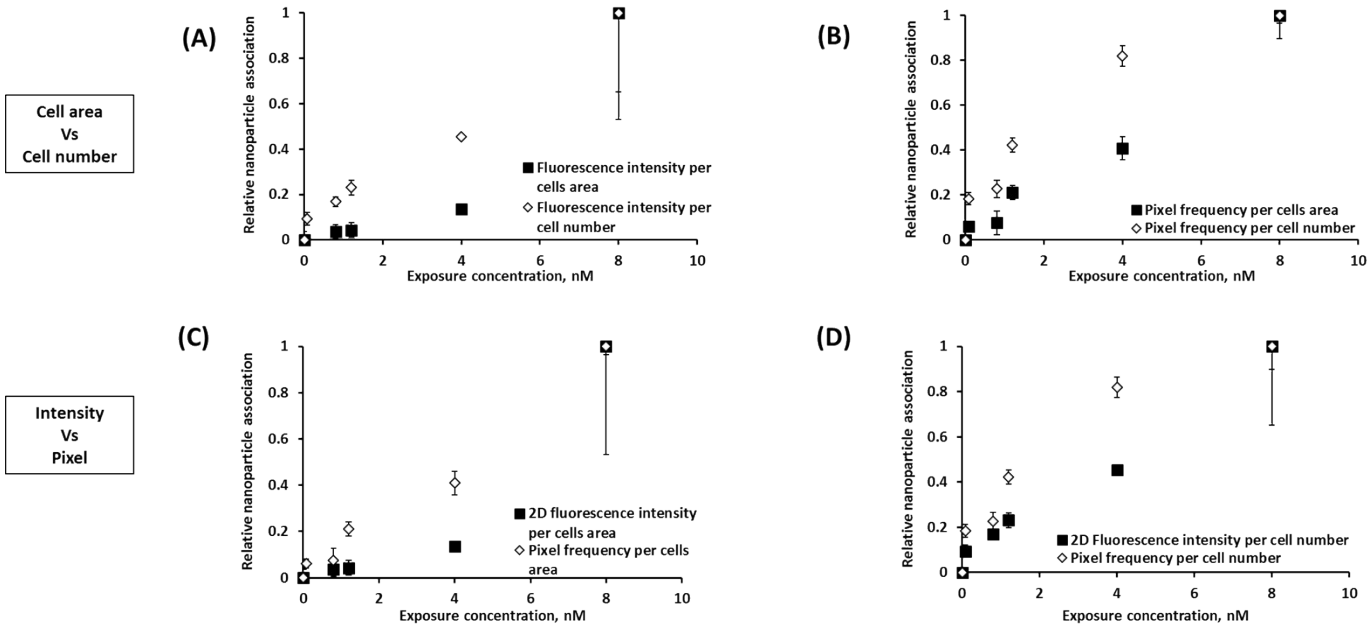

Figure S10: Effect of the method adopted for 2D image analysis of sequestered Z-stacks on the association results of labelled liposomes as determined by confocal imaging on exposure to HMVEC-C cells for 24h at 37°C; cells area versus cell number measurements (A and B), fluorescence intensity versus pixel frequency (C and D). (A) 2D Fluorescence intensities per cells area and cell number. (B) Pixel frequencies per cells area and cell number. (C) 2D Fluorescence intensity and pixel frequency (per cells area). (D) 2D fluorescence intensity and pixel frequency (per cell number). Points with error bars represent mean ± standard deviation. The differences between the two curves in all panels are statistically significant (Two-way ANOVA, $p<0.05$).

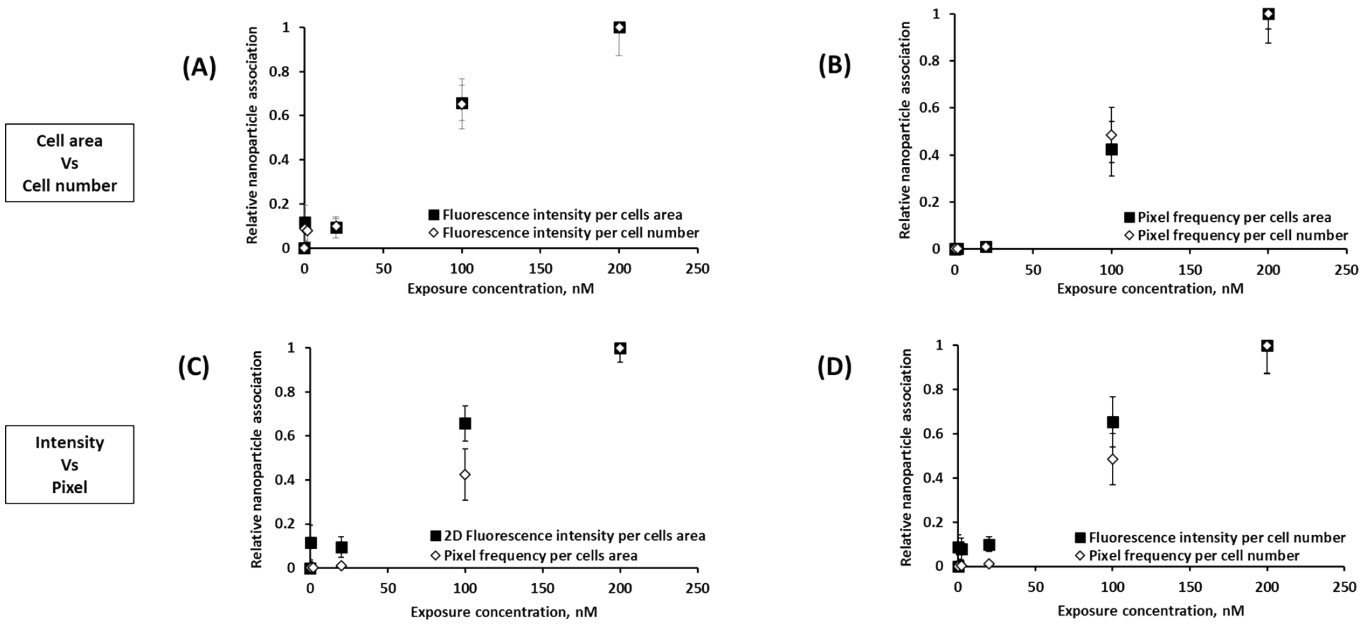

Figure S11: Effect of the method adopted for 2D image analysis of sequestered Z-stacks on the association results of quantum dots as determined by confocal imaging on exposure to HMVEC-C cells for 24h at 37°C; cells area versus cell number measurements (A and B), fluorescence intensity versus pixel frequency (C and D). (A) 2D Fluorescence intensities per cells area and cell number. (B) Pixel frequencies per cells area and cell number. (C) 2D Fluorescence intensity and pixel frequency (per cells area). (D) 2D fluorescence intensity and pixel frequency (per cell number). Points with error bars represent mean ± standard deviation. The differences between the two curves in panels C and D are statistically significant (Two-way ANOVA, $p<0.05$).

In order to compare both cell types; HUVEC and HMVEC-C, in regards to total association of quantum dots and labelled liposomes, we used the number of pixels per cells area and per cell number due to liposomal or quantum dot fluorescence. Results shown in Figure S12 indicate differential extents of cell-nanoparticles association based on the cell type and the analysis approach ("per cells area" versus "per cell number"). Association of quantum dots with HUVEC was significantly higher than with HMVEC-C; about four to six fold higher cell association was observed at 200nM quantum dots concentration with HUVEC than HMVEC-C cells depending on the analysis approach. For labelled liposomes, only association per cell number was significantly different among the two cell types with more than 1 fold higher association

observed with HMVEC-C at 8nM liposomal concentration.

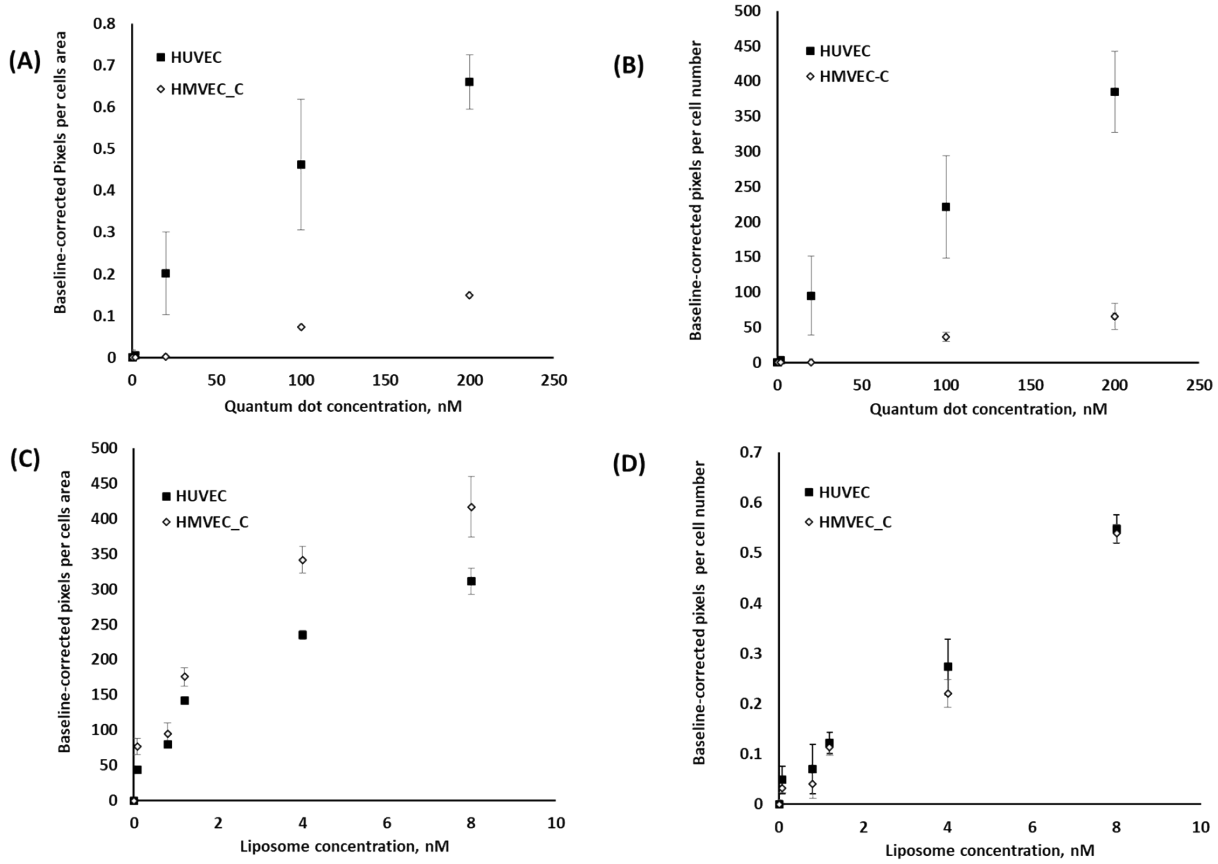

Figure S12: Effect of cell type (HUVEC AND HMVEC-C) on cell association of labelled liposomes (A and B) and quantum dots (C and D) following cell exposure for 24h at 37°C as determined by confocal images and analyzed using image J to determine the pixel counts per cell area (A and C) and per cell number (B and D).

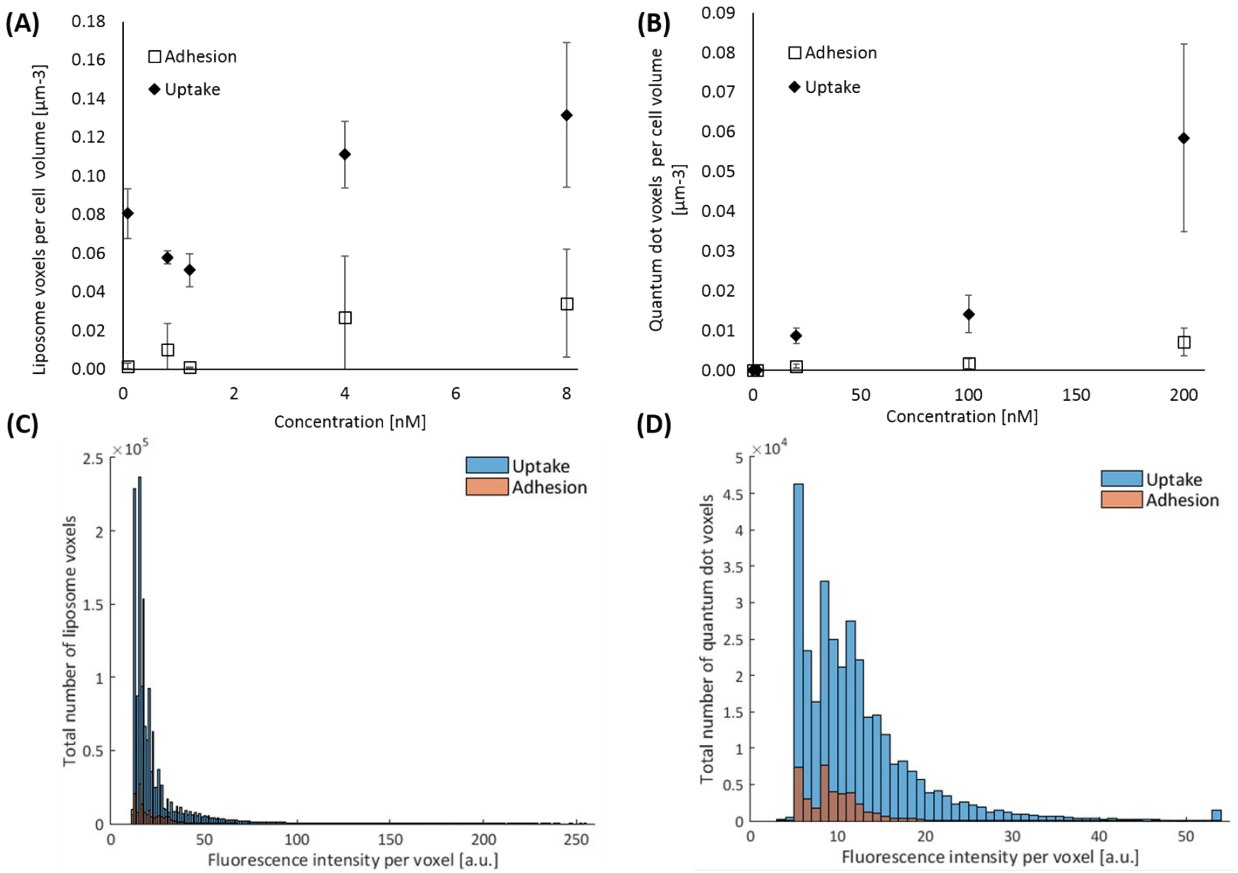

Figure S13: Quantification of liposomes (A) and quantum dots (B) by number of nanoparticle voxels in cell membrane (adhesion) and internal (uptake) of HUVECs after 24h of exposure. Adhesion and uptake both increased with increasing initial liposome concentration. Histogram showing the number of nanoparticle voxels at each level of fluorescence intensity for liposomes (C) and quantum dots (D) inside (uptake) and on the cell (adhesion). Fluorescence intensity for liposome voxels shows a wider range and dispersion than the quantum dot voxels. Results were obtained from 3D models built in ScanIP Simpleware.

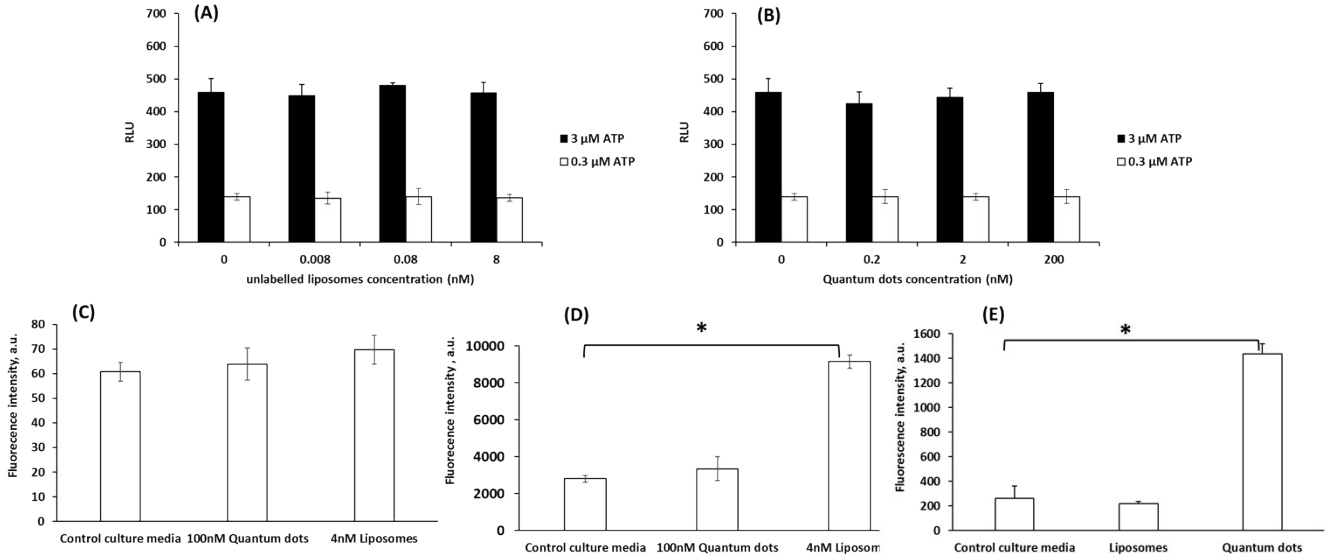

Figure S14: Interference assays for the cytotoxicity kits employed within this study; Vialight assay (A: unlabelled liposomes and B: quantum dots), CellROX kit (C), LipidTOX kit (D) and Mitohealth kit (E). Results show only interference of liposomes and quantum dots with LipidTOX and Mitohealth kits, respectively. * denotes significant difference ($p< 0.05$).

References

1. N. Nafee, M. Schneider, U. F. Schaefer and C.-M. Lehr, *International Journal of Pharmaceutics*, 2009, **381**, 130-139.
2. D. Koley and A. J. Bard, *Proceedings of the National Academy of Sciences of the United States of America*, 2010, **107**, 16783-16787.
3. A. Albanese, P. S. Tang and W. C. W. Chan, *Annual Review of Biomedical Engineering*, 2012, **14**, 1-16.
4. *Journal*, Revised: 6–May–2012, **MAN0003555**.
5. D. N. Criddle, S. Gillies, H. K. Baumgartner-Wilson, M. Jaffar, E. C. Chinje, S. Passmore, M. Chvanov, S. Barrow, O. V. Gerasimenko, A. V. Tepikin, R. Sutton and O. H. Petersen, *Journal of Biological Chemistry*, 2006, **281**, 40485-40492.
6. G. Loor, J. Kondapalli, J. M. Schriewer, N. S. Chandel, T. L. Vanden Hoek and P. T. Schumacker, *Free radical biology & medicine*, 2010, **49**, 1925-1936.
7. K. Haasio, A. Koponen, K. E. Penttilä and E. Nissinen, *European Journal of Pharmacology*, 2002, **453**, 21-26.
8. W. H. Halliwell, *Toxicologic Pathology*, 1997, **25**, 53-60.
9. T. T. Nguyen, J. L. Swift, M. C. Burger and D. T. Cramb, *The Journal of Physical Chemistry B*, 2009, **113**, 10357-10366.
10. H. I. Labouta, S. Menina, A. Kochut, S. Gordon, R. Geyer, P. Dersch and C.-M. Lehr, *Journal of Controlled Release*, 2015, **220, Part A**, 414-424.
11. E. Mayhew, M. Ito and R. Lazo, *Experimental Cell Research*, 1987, **171**, 195-202.
12. U. Leli and G. Hauser, *Biochemical Pharmacology*, 1987, **36**, 31-37.